Partitioning of Pyrene between "Crew Cut" Block Copolymer Micelles and H_2O/DMF Solvent Mixtures

Jianxi Zhao, Christine Allen, and Adi Eisenberg*

Department of Chemistry, McGill University, 801 Sherbrooke Street West, Montreal, PQ, Canada H3A 2K6

Received March 28, 1997; Revised Manuscript Received September 11, 1997[⊗]

ABSTRACT: The effect of solvent composition on the partition coefficient (K_V) of pyrene between the crew cut micelles formed from highly asymmetric block copolymers of polystyrene (500)-*b*-polyacrylic acid (60) and an H_2O/DMF solvent mixture was studied using a fluorescence method. The total number of pyrene molecules incorporated per micelle was also determined as a function of polymer concentration and solvent composition. The relationship between the partition coefficient (K_V) and the mass equilibrium constant (K) was obtained, and the free energy of transfer of pyrene from the solvent mixture to the micelle was calculated in terms of K. The results suggest that a gradual change in the solvent composition, which makes it increasingly incompatible with the solubilizate, may be a good method of loading hydrophobic materials into micelles.

Introduction

Self-assembling colloidal carriers have been receiving much attention as potential drug delivery systems.[1−5] Such systems include micelles formed either from small-molecule surfactants or from amphiphilic block copolymers. Low molecular weight surfactants are frequently considered for pharmaceutical use due to their low toxicity.[6,7] However, their application in drug delivery is restricted due to their relatively low capacity for drug loading.[11,12] Similar to surfactants, amphiphilic block copolymers with hydrophobic and hydrophilic segments are generally self-assembled in the form of micelles in aqueous media. In these micelles, the hydrophobic blocks constitute the core and the hydrophilic blocks, along with the solvent (which can have a variable water content), form the corona. Some block copolymer micelles have been studied for drug delivery; these include poly(aspartic acid)-*b*-poly(ethylene glycol),[13] poly(*β*-benzyl L-aspartate)-*b*-poly(ethylene oxide),[14] poly(oxyethylene)-*b*-poly(isoprene)-*b*-poly(oxyethylene),[15] poly(oxyethylene)-*b*-poly(oxypropylene)-*b*-poly(oxyethylene),[16] and many others.

Several laboratories have recently studied the incorporation of model hydrophobic materials by the block copolymer micelles.[17−19] Nagarajan et al.[17a] compared the solubilization of aromatic and aliphatic hydrocarbons in poly(ethylene−propylene oxide) and poly(*N*-vinylpyrrolidone−styrene) block copolymer micelles. They found that the solubilizate which is more compatible with the core-forming block is solubilized to a greater extent. A thermodynamic treatment of hydrocarbon solubilization was presented by the same group for both diblock and triblock copolymer molecules.[17b] Their results demonstrated that the core radius, the corona thickness and the aggregation number for the diblock copolymer micelles are much larger than those for the triblock copolymer micelles of identical molecular weights and block compositions. Tian et al.[18] determined the solubilization of organic substances by styrene−methacrylic acid block copolymer micelles using light scattering measurements and suggested that the compounds which interact favorably with polystyrene are solubilized to a much larger extent than the compounds which interact less favorably.

Solubilization within the core is controlled by the partition coefficient of the material between the hydrophobic micellar core and the hydrophilic aqueous phase. The pharmacokinetic behavior of the system in terms of controlled release will also depend upon this partitioning. Therefore, the partition coefficients of hydrophobic materials within micellar systems of both surfactant molecules and block copolymers have been studied by various groups. A fluorescence quenching technique developed by Auger et al.[8] enabled measurement of the napthalene partition coefficient in aqueous solutions of nonionic surfactant micelles. One significant benefit of using this technique is that the partitioning of napthalene can be determined for both saturated and unsaturated solutions. Itoh et al.[9] used fluorescence measurements to determine the partition coefficient of pyrene in aqueous solutions of *n*-*β*-octylglucoside micelles. They also calculated the free energy of transfer of pyrene from the solvent water phase to the micellar cores.

Moroi et al.[10] compared the solubilization of several cyclic aromatic hydrocarbons in 1-dodecanesulfonic acid micelles. They found that the first stepwise association constant increased in order from benzene to naphthalene to anthracene to pyrene. These studies clearly indicate that control over solubilization is largely exerted by hydrophobic interactions between the solubilizate and the micelle core.

Pyrene partitioning between the poly(styrene−ethylene oxide) block copolymer micellar phase and the water phase was studied by Wilhelm et al. using fluorescence measurements.[19] The partition coefficient of pyrene was found to have a value of the order of 10^5. In a previous paper from this laboratory, the partition coefficient of pyrene between the polystyrene-*b*-poly(acrylic acid) block copolymer micelles and water phase was also reported to be on the order of 10^5.[20] Hurter and Hatton[21] examined the partitioning of three polycyclic aromatic hydrocarbons, naphthalene, phenanthrene, and pyrene, between water and micelles formed by poly(ethylene oxide−propylene oxide) block copolymers. The micelle−water partition coefficient was found to increase with both an increase in the polypropylene oxide content of the copolymer and with an increase in the molecular weight. Kabanov et al. suggested an ap-

* To whom correspondence should be addressed.

[⊗] Abstract published in *Advance ACS Abstracts,* November 1, 1997.

S0024-9297(97)00427-0 CCC: $14.00

proach for the calculation of the partition coefficient from the emission spectrum of pyrene between Pluronic micelles of poly(oxyethylene-*b*-oxypropylene-*b*-oxyethylene) triblock copolymers and bidistilled water.[16]

Crew cut micelles have recently been the subject of extensive research in this laboratory.[22−26] The crew cuts are formed from amphiphilic block copolymer chains with long hydrophobic core forming blocks and short hydrophilic blocks.[22] The long hydrophobic blocks make it impossible to prepare micelles by simply dissolving the block copolymer in water. Therefore a method of preparation is adopted which involves dissolving the block copolymer in a common solvent for both blocks (e.g. DMF) and then slowly adding a precipitant for the hydrophobic block (e.g. water). The crew cut micelle earned its name due to its thin hydrophilic brushlike shell which surrounds a large hydrophobic core. The crew cut micelles as a drug delivery system may have an enhanced capacity for the solubilization of nonpolar drugs due to their large hydrophobic cores. In this study, the polystyrene-*b*-polyacrylic acid micelles serve as a model crew cut system and pyrene as the model for a hydrophobic drug.

In this communication we report on the calculation of the partition coefficient (K_V) of pyrene between crew cut micelles of polystyrene-*b*-polyacrylic acid and an H_2O/DMF solvent mixture. We examine the effect of water content in the solvent mixture on both the total amount of pyrene incorporated into micelles and the number of molecules incorporated per micelle. The relationship between the partition coefficient (K_V) and the mass equilibrium constant (K) is obtained, and the free energy of transfer of pyrene from the solvent mixture to the micelles is given in terms of K.

Theoretical Aspects

1. Fluorescence. Wilhelm et al.[19] and Kabanov et al.[16] suggested different fluorescence methods to calculate the partition coefficient for pyrene in micellar solutions. The approach described by Wilhelm et al.[19] is based on monitoring changes in the intensity ratio $I_{338}/I_{332.5}$ in the excitation spectrum of pyrene. The method proposed by Kabanov et al.[16] involved examination of the fluorescence emission intensity of pyrene at $\lambda = 395$ nm. Our fluorometric approach is a hybrid version of these methods with a few minor modifications. We monitor changes in the intensity of the third vibrational band and the first vibrational band (I_3/I_1) in the emission spectrum of pyrene in various DMF/H_2O solvent mixtures. The I_3/I_1 ratio is used to calculate both the amount of pyrene absorbed into the micelle cores, the number of pyrene molecules per micelle and the partition coefficient of pyrene. The partition coefficients determined this way are then used to recalculate the I_3/I_1 ratios, the amount of pyrene absorbed and the number of pyrene molecules per micelle. A comparison of the experimental and recalculated I_3/I_1 ratios will enable a check of the self-consistency of the approach. This will also enable any shortcomings or breakdowns which may arise through the use of this fluorescence method to be revealed.

2. Pyrene Monomer Fluorescence. Pyrene has commonly been used as a hydrophobic fluorescence probe, to evaluate the polarity of various environments.[9,27,28] The fluorescence emission spectrum of pyrene shows some vibrational bands which are affected by the polarity of the surrounding environment of the probe molecules. Specifically, changes in the relative intensity of the first and third vibrational bands in the pyrene emission spectrum have proven to be reliable tools in examining the polarity of the microenvironment.[9,27,28]

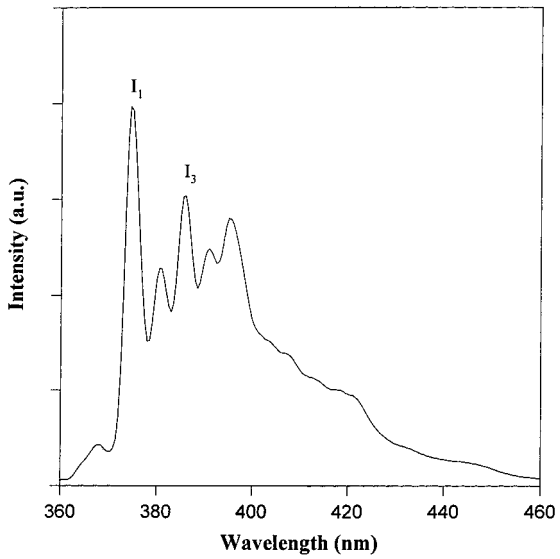

Figure 1. Fluorescence emission spectrum of pyrene (1.5×10^{-9} mol/g) in 85%/15% H_2O/DMF at a copolymer concentration of 5.6×10^{-4} g/g.

Figure 1 presents the monomer fluorescence spectrum for pyrene in aqueous solution (pyrene concentration = 1.5×10^{-9} mol/g). The concentration is low to avoid excimer formation. As is customary, the five predominant peaks or vibrational bands in the spectrum are numbered from left to right as one to five. The first vibrational band (0−0 band) shows a significant intensity variation in response to changes in polarity; for instance, considerable intensity enhancement is observed in a polar solvent. The third vibrational band demonstrates only a minimal intensity variation in response to changes in microenvironment polarity. Thus, the intensity ratio of vibrational band three to vibrational band one, i.e., the intensity of peak three normalized with reference to peak one, is strongly related to the polarity of the surrounding medium of the pyrene.

3. Calculation of the Amount of Pyrene Absorbed. The intensity of fluorescence emission (I) at wavelength λ may be written as

$$I = k\phi(1 - 10^{-\epsilon_\lambda l[\mathrm{Py}]}) = K_a\phi\epsilon_\lambda[\mathrm{Py}] \qquad (1)$$

where $K_a = kl \times \ln 10$ k is an instrumental constant, l is the cell path length, ϵ_λ is the molecular decadic extinction coefficient at wavelength λ, ϕ is the quantum yield, and [Py] = the total concentration of pyrene = $[\mathrm{Py}]_M + [\mathrm{Py}]_V$, where $[\mathrm{Py}]_M$ is the concentration of pyrene in micelles and $[\mathrm{Py}]_V$ is the concentration of pyrene in the solvent.

For pyrene in a copolymer micellar solution, the fluorescence intensity of the third vibrational band is[16,19]

$$I_3^U = K_a(\phi_V\epsilon_{3,V}[\mathrm{Py}]_V + \phi_M\epsilon_{3,M}[\mathrm{Py}]_M)$$

$$= K_a(\phi_V\epsilon_{3,V}[\mathrm{Py}] + (\phi_M\epsilon_{3,M} - \phi_V\epsilon_{3,V})[\mathrm{Py}]_M) \qquad (2)$$

where the superscript U refers to the micellar solution.

For the same concentration of pyrene in the same solvent mixture in the absence of copolymer, the emission intensity (I_3^V) may be described as:

$$I_3^V = K_a \phi_V \epsilon_{3,V} [Py] \quad (3)$$

Thus

$$\frac{I_3^U - I_3^V}{I_3^V} = \frac{\phi_M \epsilon_{3,M} - \phi_V \epsilon_{3,V}}{\phi_V \epsilon_{3,V}} \frac{[Py]_M}{[Py]}$$

$$= \left(\frac{\phi_M \epsilon_{3,M}}{\phi_V \epsilon_{3,V}} - 1 \right) \frac{[Py]_M}{[Py]}$$

$$= \left(\frac{I_{3,max}}{I_{3,min}} - 1 \right) \frac{[Py]_M}{[Py]} \quad (4)$$

where $I_{3,max}$ is the fluorescence intensity when all the pyrene is in the micelle cores and $I_{3,min}$ is the fluorescence intensity when all the pyrene is in the solvent. If both $I_{3,max}$ and $I_{3,min}$ are known, the absorbed amount of pyrene in the micelles may be calculated.

4. Calculation of I_3^U from the Partition Coefficient. Wilhelm et al.[19] suggested that pyrene binding to the micelles may be described as a simple partition equilibrium between a micellar phase and a solvent phase. They provided an equation to describe the relationship between the partition coefficient (K_V) and the ratio of pyrene in the micellar phase to pyrene in the solvent phase

$$\frac{[Py]_M}{[Py]_V} = \frac{K_V \chi_{PS} C}{\rho_{PS}} \quad (5)$$

where χ_{PS} is the weight fraction of polystyrene in the polymer, ρ_{PS} is the density of the polystyrene core of the micelle, and C is the concentration of polymer in g/mL. In this expression, the measurements are assumed to be insensitive to micellar association of polymer molecules.

From eq 5, we get

$$\frac{[Py]_M}{[Py]} = \frac{K_V \chi_{PS} C}{\rho_{PS} + K_V \chi_{PS} C} \quad (6)$$

Substituting into eq 4 and rearranging

$$I_3^U = \left(\frac{I_{3,max}}{I_{3,min}} - 1 \right) \frac{K_V \chi_{PS} C}{\rho_{PS} + K_V \chi_{PS} C} I_3^V + I_3^V \quad (7)$$

In this way, we can theoretically calculate I_3^U from the measured partition coefficient K_V. The absorbed amount of pyrene can also be calculated in terms of the measured partition coefficient K_V using eq 6.

5. Relationship between K_V and K. Hunter[29] suggested a kinetic approach with

$$M_{n-i} + A \leftrightarrow M_n \quad (8)$$

to describe the distribution of probe molecule A between the micelles and the solvent phase, where M_n is a micelle containing n probe molecules and A is a probe molecule in the surrounding solvent. In the present case, A = Py (pyrene).

If there is no limit to the number of solubilized molecules per micelle, then the mass equilibrium constant, K, of the distribution of pyrene molecules is

$$K = \frac{[Py]_M}{C^\circ_M [Py]_V} \quad (9)$$

where $[Py]_M$ and $[Py]_V$ are the pyrene concentrations in the micelle and in the solvent phase, respectively. C°_M is the micellar concentration, i.e.

$$C^\circ_M = \frac{(C - cmc)}{N} \quad (10)$$

where C is the concentration of polymer, cmc is the critical micelle concentration, and N is the aggregation number. The cmc for this block copolymer is extremely small, it has been reported to be on the order of 10^{-7} with a 4.5 wt % water content.[30] If the water content is extrapolated to 15 wt % the cmc value at 25 °C is ca. 1×10^{-24} M and will decrease further as more water is added.[30] Equation 10 thus becomes

$$C^\circ_M \cong \frac{C}{N} \quad (11)$$

Substituting both eq 11 and eq 5 into eq 9, we get

$$K = \frac{N K_V \chi_{PS}}{\rho_{PS}} \quad (12)$$

From this equation, the mass equilibrium constant K can be calculated through the partition coefficient K_V if the aggregation number N is known.

6. Calculation of Free Energy of Transfer. From the mass equilibrium constant K, we have

$$\Delta G^\circ = -RT \ln K \quad (13)$$

where ΔG° is the free energy of transfer of pyrene molecules from the solvent phase to the micelles.

Experimental Section

Materials. The block copolymer used was polystyrene-*b*-poly(acrylic acid) (PS(500)-*b*-PAA(60)) containing 500 styrene repeat units and 60 acrylic acid repeat units. This block copolymer was synthesized by sequential anionic polymerization of styrene monomer followed by *tert*-butyl acrylate monomer. The polymerization process was carried out in tetrahydrofuran (THF) at −78 °C under nitrogen gas. Before the addition of *tert*-butyl acrylate monomer, an aliquot of the reaction medium was withdrawn to obtain the styrene chain, which had a polystyrene chain length identical to that in the diblock copolymer which was to be synthesized subsequently. A more detailed description of the procedures was given in a previous communication.[31] The block copolymer had a narrow distribution of molecular weights, and the polydispersity index (M_w/M_n), estimated by gel permeation chromatography (GPC), was 1.04. The synthesized block copolymers were hydrolyzed to the acid form (PS-*b*-PAA) in toluene at 110 °C reflux overnight by using *p*-toluenesulfonic acid as the catalyst (5 mol % relative to the polyacrylate content). Pyrene was purchased from Aldrich Chemical (USA) and was recrystallized two times in ethanol.

Preparation of Solutions. Sample solutions were prepared by adding known amounts of pyrene in acetone to each of a series of empty flasks, after which the acetone was evaporated. The amount of pyrene was chosen so as to give a pyrene concentration in the final solution of 1.5×10^{-9} mol/g. Different amounts of polymer in *N*,*N*-dimethylformamide (DMF) were then added. The initial volumes of the solutions were *ca.* 2 mL. Micellization of the polymer was achieved by adding water at a rate of 1 drop every 10 s. The addition of water was continued until the desired water content was reached. The polystyrene-*b*-poly(acrylic acid) block copolymer used here was found to have a very low cmc and to form

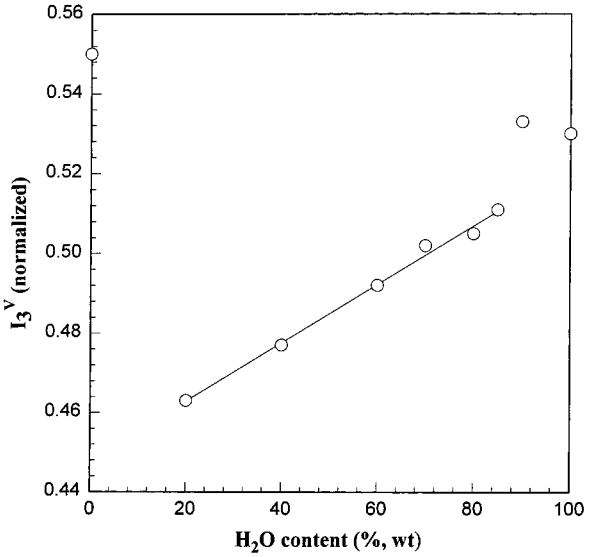

Figure 2. Intensity (I_3^V) as a function of water content in the solvent mixture in the absence of copolymer. Pyrene concentration = 1.5×10^{-9} mol/g.

spherical micelles with an aggregation number of 160 when water content added exceeds 5%.[24,30] All the sample solutions were stirred overnight before fluorescence measurement.

Fluorescence Measurements. Steady-state fluorescent spectra were measured using a SPEX Fluorolog 2 spectrometer in the right-angle geometry (90° collecting optics). For the fluorescence measurements, 3 mL of solution was placed in a 1.0-cm square quartz cell. All spectra were run on air-equilibrated solutions. For fluorescence emission spectra, λ_{ex} was 339 nm, and for excitation spectra, λ_{em} was 390 nm. Spectra were accumulated with an integration time of 1 s/0.5 nm.

Results and Discussion

1. Pyrene in the Solvent Mixture. The effect of water content in the solvent mixture on the intensity ratio of peak 3/peak 1 (i.e., I_3 normalized to I_1; here we simply represent it as I_3^V, where V means solvent) in the absence of polymer, is shown in Figure 2. With increasing water content, I_3^V is enhanced. Generally, the peak ratio is affected by two factors: the dipole moment of the solvent and its dielectric constant.[28] When the dipole moment of the solvent decreases, the peak ratio increases, and for any two given solvents with the same dipole moment, the one with the smaller dielectric constant has the higher peak ratio. On the basis of these premises, Kalyanasundaram and Thomas[28] gave a larger value for the I_3/I_1 peak ratio in water than in DMF, which is in agreement with our result. In the present case, a linear relationship between I_3^V and water content was found over the range of 20−85% water content (see Figure 2). At 90% water, a sharp increase in I_3^V was observed. The value in pure water is 0.53, while that in pure DMF is 0.55.[27]

2. Pyrene Partitioning in Micellar Solutions. It should first be noted, that the experimental points in Figures 3−5 will be discussed now in sections 2 and 3 while the lines found in these figures will be discussed later in section 5. The experimental points in Figure 3 show the normalized I_3^U as a function of polymer concentration. The measured values of I_3^U (symbols) reveal changes with both the polymer concentration and the solvent composition. In all cases the polymer concentration is far above that of the cmc for this diblock copolymer.[30] It is seen that with an increase in polymer

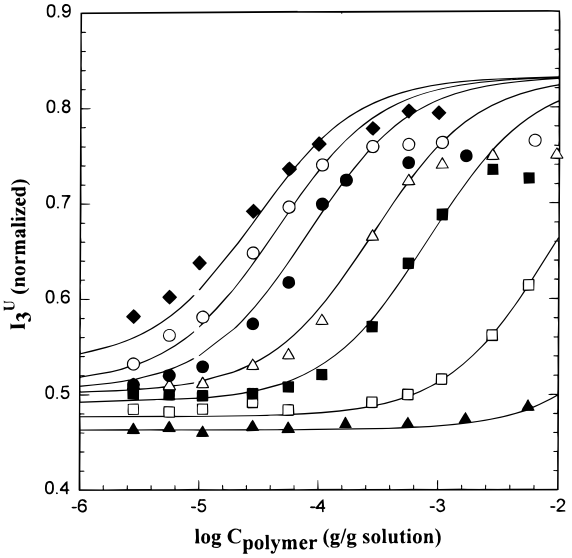

Figure 3. Semilogarithmic plots of the fluorescence intensity (I_3^U) as a function of polymer concentration in different solvent mixtures. Symbols represent the experimental values for the various solvent mixtures expressed as % H_2O/% DMF: (◆) 90/10, (○) 85/15, (●) 80/20, (△) 70/30, (■) 60/40, (□) 40/60, and (▲) 20/80. The curves were calculated using eq 7.

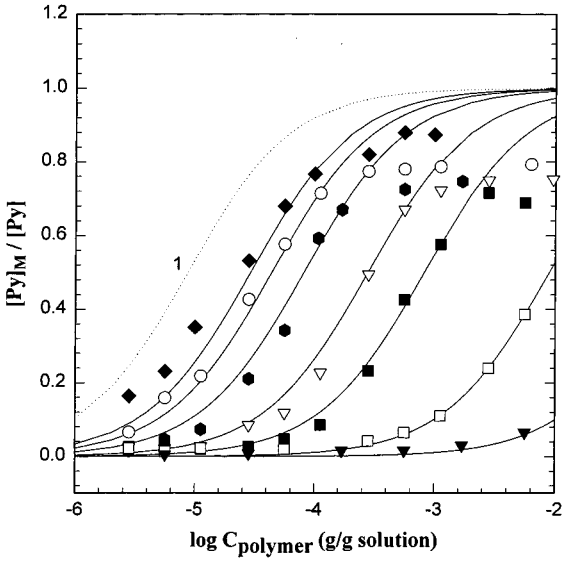

Figure 4. Semilogarithmic plots of $[Py]_M/[Py]$ vs copolymer concentration in different solvent mixtures. Symbols represent the experimental values for the various solvent mixtures expressed as % H_2O/% DMF: (◆) 90/10, (○) 85/15, (●) 80/20, (▽) 70/30, (■) 60/40, (□) 40/60, and (▼) 20/80. The curves were calculated using eq 6.

concentration, the I_3^U increases until it reaches a plateau. In a micellar solution, the I_3^U reflects the combined contributions of both the pyrene molecules in the micellar cores and those in the solvent phase. It is well known that the peak 3/peak 1 intensity ratio has a larger value for pyrene in a hydrophobic environment in comparison to that in a hydrophilic one.[9,27,28] Thus, the increase in I_3^U means that more pyrene molecules are incorporated into the micelles with increasing polymer concentration. However, I_3^U remains small but almost constant over the range of low polymer concentration, particularly in the solvent mixture with low water contents.

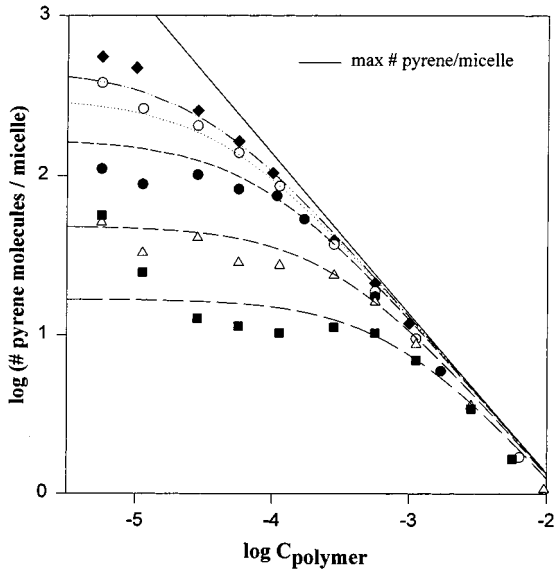

Figure 5. Logarithmic plot of the number of pyrene molecules per micelle as a function of polymer concentration for the various DMF/H_2O solvent mixtures. Key: (– ·· –, ◆) 90% H_2O; (···, ○) 85% H_2O; (- -, ●) 80% H_2O; (– –, △) 70% H_2O; (— —, ■) 60% H_2O.

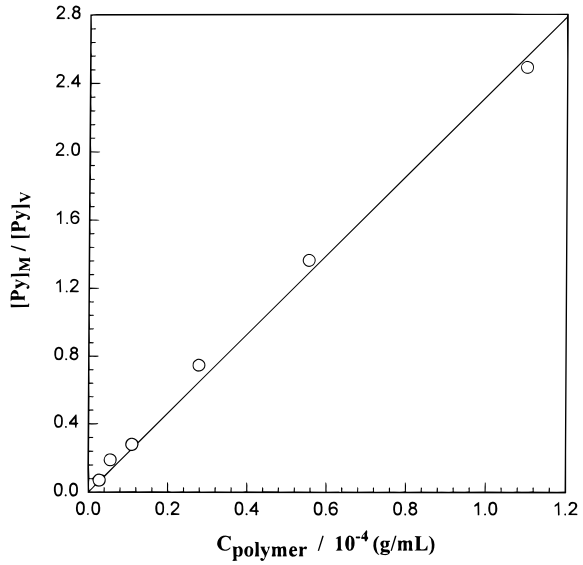

Figure 6. Plot of $[Py]_M/[Py]_V$, obtained from fluorescence data, vs copolymer concentration in g/mL for the 85%/15% H_2O/DMF mixture. From this plot the partition coefficient of pyrene calculated by eq 5.

At a constant concentration of polymer, I_3^U increases with increasing water content in the solvent mixture. Solvent mixtures with higher water contents have a significantly lower capacity to accommodate pyrene molecules, and more solute is thus incorporated into the micelle cores, leading to an increase in I_3^U. This result suggests that an increase in solvent polarity may be a simple preparative method to achieve a high loading of hydrophobic solubilizate.

3. Calculation of the Amount of Pyrene Absorbed. In order to calculate the amount of absorbed pyrene using eq 4, the two parameters, $I_{3,min}$ and $I_{3,max}$, must first be obtained. Here we chose the I_3^V value (Figure 2) measured in the solvent mixture with 1.5×10^{-9} mol/g of pyrene in the absence of copolymer to be equivalent to $I_{3,min}$ for the corresponding micelle solution.

In the polymer micellar solutions, as previously described, the total fluorescence intensity I_3^U is a result of combined contributions of pyrene molecules in the micelles and in the solvent mixture. Since the saturation solubility of pyrene in water is very low (1.2×10^{-7} M at 22 °C[19]), the contribution to the pyrene fluorescence in the aqueous micellar solution, at the highest polymer concentrations, is predominantly due to pyrene in the micelle cores. Therefore in order to obtain an upper limit $I_{3,max}$ value the series of plateau values of I_3^U at the highest polymer concentrations were plotted as a function of water content in the solvent mixture and were then extrapolated to 100% water content. The value of 0.83 was obtained as the present upper limit for $I_{3,max}$.

Figure 4 shows a semilogarithmic plot of the fraction of pyrene incorporated in the micelles, expressed as $[Py]_M/[Py]$, as a function of the logarithm of the polymer concentration, for each solvent mixture. The experimental data show that the absorbed amount of pyrene increases for increasing polymer concentrations. Since the solutions used are all above the cmc, increasing the polymer concentration results in an increase in the number of micelles in solution. Clearly, the total number of pyrene molecules incorporated increases as more micelles are present. However, as the number of micelles is increased, the ratio of the total number of pyrene molecules per micelle is decreased. This is clearly seen in Figure 5, the logarithmic plot of the number of molecules per micelle as a function of polymer concentration for the various solvent mixtures. The diagonal line (in Figure 5) represents the ratio of the total number of pyrene molecules per micelle if one assumes that all molecules are incorporated into the micelles. The diagonal line shows that the maximum possible number of pyrene molecules per micelle decreases linearly on a log–log plot as the polymer concentration is increased. The experimental points in Figure 5 show that each micelle solution reaches a maximum number of molecules per micelle at a different polymer concentration, depending on the water content in the solvent mixture. The greater the water content in the solvent mixture, the lower the polymer concentration required to reach the maximum number of molecules per micelle. Another phenomenon that is worth noting is that the 60, 70, and 80% water content solutions have a fairly wide plateau region over which the number of molecules incorporated is independent of the polymer concentration. This plateau extends over one magnitude of polymer concentration (1×10^{-5} to 1×10^{-4} g/g) and the plateau value increases with increasing water content such that for the 60% solution the plateau is seen at 10 molecules/micelle while for the 70% solution it is at 32 molecules/micelle and for the 80% it is at 100 molecules/micelle. This is quite interesting when it is considered that over this concentration range the number of micelles present in solution has increased by an order of magnitude, yet the number of pyrene molecules per micelle remains practically constant.

4. Partition Coefficient. The $[Py]_M/[Py]_V$ values for each solvent mixture were obtained from the fluorescence data are plotted against copolymer concentration. Figure 6 shows the $[Py]_M/[Py]_V$ vs copolymer concentration plot for the 85/15% H_2O/DMF solvent mixture; such plots were made for each solvent mixture. The slope of figure 6 is used in the calculation of the partition coefficient K_V in terms of eq 5, as suggested by Wilhelm et al.[19] Figure 7 shows a semilogarithmic

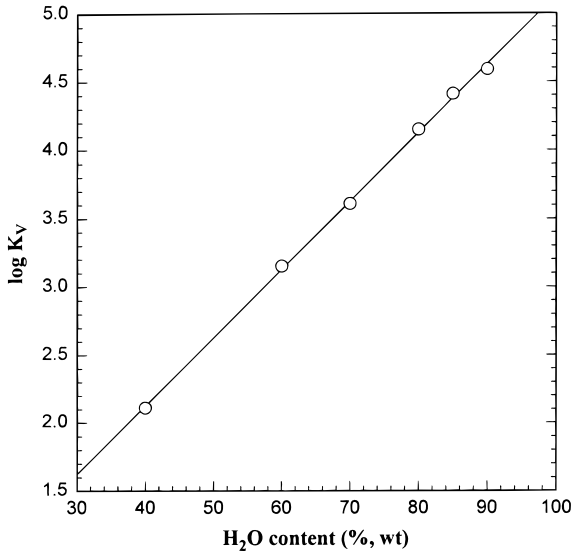

Figure 7. A semilogarithmic plot of partition coefficient (K_V) vs water content in the solvent mixture.

plot of the partition coefficient as a function of water content in the solvent mixture. K_V increases with increasing water content in the solvent mixture. The dependence of log K_V on solvent composition is seen to be linear. For pure water, K_V is 1.3×10^5 calculated from this linear relationship. This value is close to that reported by Wilhelm et al[19] who suggested that the K_V values range from 2×10^5 to 4×10^5 for pyrene partitioning between the micelles of polystyrene−poly(ethylene oxide) diblock and poly(ethylene oxide)−polystyrene−poly(ethylene oxide) triblock copolymers and the water phase. We previously obtained similar values for K_V, ranging from 1.9×10^5 to 2.5×10^5, for pyrene partitioning between the micelles of polystyrene-*b*-poly(acrylic acid) diblock copolymers and water.[20]

In the solvent mixture of 50% water content. K_V equals 4.2×10^2, which is 1000 times smaller than that in aqueous solution. This again demonstrates the strong influence of solvent environment on the partitioning of pyrene between the micellar and solvent phases.

5. Calculation of I_3^U, $[Py]_M/[Py]$, and Pyrene Molecules/Micelle. Knowing the value of K_V as a function of water content, we are now able to calculate *a priori* the plots for I_3^U, $[Py]_M/[Py]$, and the number of molecules/micelle for a range of polymer concentrations (1×10^{-6} to 1×10^{-2}) in solvents of variable water content. The calculations are described below and plots are shown as the lines in Figures 3−5.

5.1. Calculated Values of I_3^U. Using the upper limit value for $I_{3,max}$ and the respective values for $I_{3,min}$, the curves were calculated by eq 7 and are shown in Figure 3. They are in good agreement with the experimental data over the range of low and medium polymer concentrations (1×10^{-6} to 1×10^{-4}). However, there is a deviation in the plateau region found at high polymer concentrations. One possible interpretation of the deviation is given in section 5.1.2.

5.1.1. Low Polymer Concentration Region. At low polymer concentrations, the calculated curves obtained using eq 7 and the upper limit $I_{3,max}$ value fit the experimental points quite well. The calculated values match the I_3^U experimental values which approach the $I_{3,min}$ values for each solvent mixture. The agreement between the $I_{3,min}$ calculated and experimental values at low polymer concentrations may be explained as follows: In the present case, the density of polystyrene is close to 1 ($\rho_{PS} = 1.04$ g/mL). When the polymer concentration is very low, the fraction term in the right hand side of eq 7 may be simplified to

$$\frac{K_V\chi_{PS}C}{\rho_{PS} + K_V\chi_{PS}C} \approx \frac{K_V\chi_{PS}C}{\rho_{PS}} \tag{14}$$

Thus, since $K_V\chi_{PS}C \ll 1$ and $\rho_{PS} \approx 1$, thus $I_{3,max}/I_{3,min} \gg 1$, and I_3^U becomes

$$I_3^U \approx I_{3,max}K_V\chi_{PS}C + I_{3,min} \approx I_{3,min} \tag{15}$$

As described above, the I_3^V was adopted as the corresponding $I_{3,min}$. For solvents of low water content, when the polymer concentration is very low, the majority of the pyrene molecules remain in the solvent phase. Thus, the contribution of pyrene to the fluorescence intensity arises mainly from pyrene in the solvent phase.

5.1.2. High Polymer Concentration Region. When the polymer concentration is very high, the fraction term

$$\frac{K_V\chi_{PS}C}{\rho_{PS} + K_V\chi_{PS}C} \approx 1 \tag{16}$$

We therefore have

$$I_3^U \approx I_{3,max} \tag{17}$$

Therefore, the calculated curves reach a plateau at the value of $I_{3,max}$ as shown in Figure 3. The $I_{3,max}$ plateau value describes the intensity of emission when all of the pyrene is in the micelle core.

In Figure 3, the theoretical I_3^U curves were calculated using 0.83 as the value for $I_{3,max}$, which assumes no DMF in the core. The calculated theoretical curves deviate from the experimental points in the plateau region. This deviation seems to increase with decreasing water content. One possible explanation for this deviation is based on the premise that the $I_{3,max}$ value should not be the same for all solvent mixtures, since in each case there will be a different amount of DMF in the polystyrene core. With this in mind, the calculated curves were then recalculated using $I_{3,max}$ values which ranged from the individual plateau values for each solvent mixture curve to the maximum extrapolated value of 0.83. It was found (Figure 8) that the lower limit $I_{3,max}$ value yields a calculated curve that is in agreement with the experimental points at higher polymer concentrations. However, the calculated $I_{3,max}$ curve recalculated using the upper limit $I_{3,max}$ value is in good agreement with experimental points obtained at lower polymer concentrations. Thus for each solvent mixture, the experimental points are best fit by one calculated curve at low polymer concentrations and another at high polymer concentrations. However, the polymer concentration at which point the crossover occurs between the experimental data being best fit by one calculated curve to another varies for each solvent mixture. As the water content in the solvent mixture is increased, the polymer concentration at which point this change occurs is decreased. Interestingly, the polymer concentration at this point of variation appears

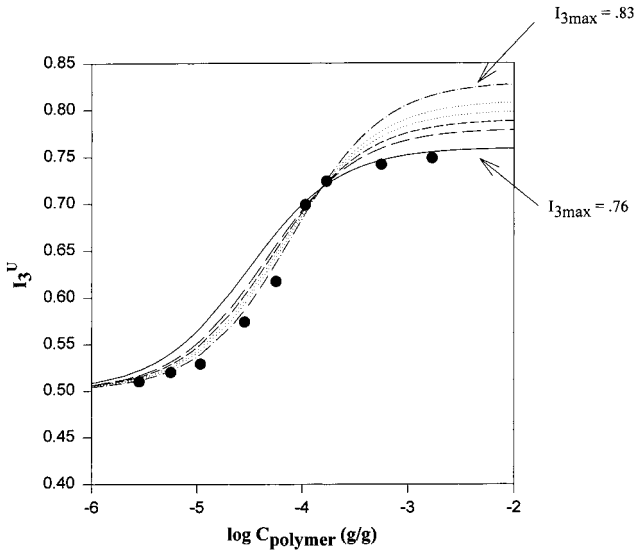

Figure 8. Semilogarithmic plots of the fluorescence intensity (I_3^U) as a function of polymer concentration for the 80%/20% H_2O/DMF solvent mixture. Symbols represent the experimental values. The curves were calculated using eq 7, for a range of values of $I_{3,max.}$

to coincide with the polymer concentration at which the experimental points approach the diagonal line in Figure 5.

The calculated curves for the fraction of pyrene incorporated into the micelles (Figure 4) were also calculated by eq 6, from the obtained partition coefficients (Figure 7). Naturally, these curves follow the same pattern as the I_3^U calculated curves.

5.2. Calculated Number of Pyrene Molecules/ Micelle. From the partition coefficients, the number of pyrene molecules incorporated per micelle in each polymer solution has been recalculated using eq 6. The recalculated values (shown as the lines in Figure 5) are in good agreement with the experimental points at high polymer concentrations (1×10^{-4} to 1×10^{-2} g/g). However the recalculated values deviate from the experimental points at low polymer concentrations (1×10^{-6} to 1.5×10^{-4} g/g). This deviation is most pronounced for the solutions having the 60% and 70% water contents.

6. Mass Equilibrium Constant and Free Energy of Transfer. In the present system, the aggregation number of the micelles is known to be 160.[24] The mass equilibrium constant (K) can thus be calculated in terms of eq 12, and is shown in Figure 9 as a function of water content in the solvent mixture. From the equilibrium constant, the corresponding free energies ($\Delta G°$) of transfer of pyrene from the solvent phase to the micelle cores were calculated by eq 13 and are shown in Figure 9. $\Delta G°$ decreases linearly with increasing water content and thus is driving the increased incorporation of pyrene into the micelle cores. Moroi et al.[10] indicated that the solubilization was controlled mainly by hydrophobic interaction between the solubilizates and the micellar cores. An increase in the hydrophobicity of the blocks which constitute the cores of micelles will generally improve solubilization.[32−34] The present results suggest further that a change in solvent composition such that it is made increasingly incompatible with the solubilizate will also enhance solubilization. This may be a convenient method to maximize the loading of hydrophobic materials into micelle cores.

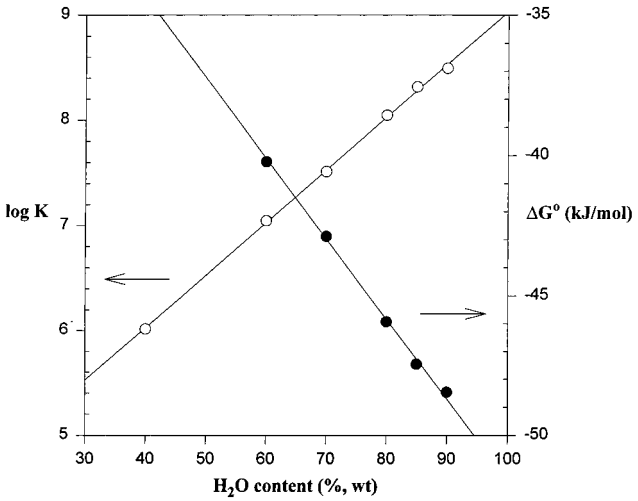

Figure 9. Semilogarithmic plot of the mass equilibrium constant (K) and the linear plot of the free energy ($\Delta G°$) of pyrene transfer from solvent phase to the micellar cores as functions of water content in the solvent mixture.

Conclusions

The partitioning of pyrene between the crew cut micelles of polystyrene-*b*-poly(acrylic acid) and the H_2O/DMF solvent mixture was studied as a function of both polymer concentration and water content in the solvent mixture. The fluorescence measurement of I_3^U enabled determination of the amount of pyrene absorbed, the number of pyrene molecules incorporated per micelle and also K_V. It was found that since log K_V increased linearly with increasing water content the total amount of pyrene incorporated into micelles also increases. The number of pyrene molecules per micelle was found to vary with both solvent composition and polymer concentration.

In the second part of the paper using only the value of K_V and its variation with water content, we calculated *a priori* I_3^U the amount of pyrene absorbed and the number of pyrene molecules incorporated per micelle. The experimental values obtained were then compared with the theoretically calculated values in order to assess the overall consistency of the fluorescence method. As described, deviations were found at the extreme high polymer concentrations between the two sets of values of I_3^U and at the extreme low concentrations for the values of pyrene molecules incorporated per micelle.

In addition, K_V was used to calculate the equilibrium constant (K), which in turn enabled the calculation of the free energy of transfer ($\Delta G°$) of pyrene from the solvent phase to the micelle phase. The free energy of transfer ($\Delta G°$) was shown to decrease with increasing water content in the solvent mixture as expected. It thus appears that the loading of hydrophobic materials into micelles may be enhanced by gradually changing the solvent composition such that it becomes increasingly incompatible with the solubilizate.

Acknowledgment. The authors thank Dr. Lifeng Zhang for the PS-*b*-PAA sample and Ms. Kui Yui for her helpful input. This research was supported by the NSERC.

References and Notes

(1) Lawrence, M. J. *Chem. Soc. Rev.* **1994**, 417.
(2) Yokoyama, M. *Crit. Rev. Ther. Drug Carrier Syst.* **1992**, *9*, 213.

(3) Ottenbrite, R. M.; Fadeeva, N. Polymer Systems for Biomedical Applications an Overview. In *Polymeric Drugs and Drug Administration* Ottenbrite, R. M., Ed.; Americal Chemical Society: Washington, DC, 1994.
(4) Kwon, G. S.; Kataoka, K. *Adv. Drug Delivery Rev.* **1995**, *16*, 295.
(5) Kabanov, A. V.; Alakhov V. Y. Micelles of Amphiphilic Block Copolymers as Vehicles for Drug Delivery. In *Amphiphilic Block Copolymers: Self-Assembly and Applications*; Alexandris P., Lindman B., Eds.; Elsevier: Amsterdam, 1997.
(6) Attwood, D.; Florence, A. T. *Surfactant Systems. Their Chemistry, Pharmacy and Biology*; Chapman and Hall: London, 1983.
(7) Florence, A. T. *Techniques of Solubilization of Drugs*; Yalkowsky, S. H. Ed.; Marcel Dekker, Inc.: New York, 1981.
(8) Auger, R. L.; Jacobson, A. M.; Domach, M. M. *Environ. Sci. Technol.* **1995**, *29*, 1273.
(9) Itoh, H.; Ishido, S.; Nomura, M.; Hayakawa, T.; Mitaku, S. *J. Phys. Chem.* 1**996**, *100*, 9047.
(10) Moroi, Y.; Mitsunobu, K.; Morisue, T.; Kadobayashi, Y.; Sakai, M. *J. Phys. Chem.* **1995**, *99*, 2372.
(11) Engstrom, S.; Lindahl, L.; Wallin, R.; Engblom, J. *Int. J. Pharm.* **1992**, *86*, 137.
(12) Wahlgren, S.; Linstrom, A. L.; Friberg, S. E. *J. Pharm. Sci.* **1984**, *73*, 1484.
(13) (a) Yokoyama, M.; Okano, T.; Sakurai, Y.; Ekimoto, H.; Shibazaki, C.; Kataoka, K. *Cancer Res.* **1991**, *51*, 3229. (b) Yokoyama, M.; Miyauchi, M; Yamada, N.; Okano, T.; Sakurai, Y.; Kataoka, K.; Inoue, S. *Cancer Res.* **1990**, *50*, 1693. (c) Yokoyama, M.; Inoue, S.; Kataoka, K.; Yui, N.; Okano, T.; Sakurai, Y. *Makromol. Chem.* **1989**, *190*, 2041. (d) Yokoyama, M.; Miyauchi, M; Yamada, N.; Okano, T.; Sakurai, Y.; Kataoka, K.; Inoue, S. *J. Controlled Release* **1990**, *11*, 269. (e) Kwon, G. S.; Suwa, S.; Yokoyama, M.; Okano, T.; Sakurai, Y.; Kataoka, K. *J. Controlled Release* **1994**, *29*, 17.
(14) (a) Kwon, G.; Maito, M.; Yokoyama, M.; Okano, T.; Sakurai, Y.; Kataoka, K. *Langmuir* **1993**, *9*, 945. (b) Kwon, G.; Maito, M.; Kataoka, K.; Yokoyama, M.; Sakurai, Y.; Okano, T. *Colloids Surf. B: Biointerfaces* **1994**, *2*, 429.
(15) Rolland, A.; O'Mullane, J.; Goddard, P.; Brookman, L.; Petrak, K. *J. Appl. Polym. Sci.* **1992**, *44*, 1195.
(16) Kabanov, A. V, Nazarova, I. R., Astafieva I. R., Batrakova E. V., Alakhov V. Y., Yarostavov A. A., Kabanov V. A. *Macromolecules* **1995**, *28*, 2303.
(17) (a) Nagarajan, R.; Barry, M.; Ruckenstein, E. *Langmuir* **1986**, *2*, 210. (b) Nagarajan, R.; Ganesh, K. *J. Colloid Interface Sci.* **1996**, *184*, 489.
(18) Tian, M.; Arca, E.; Tuzar, Z.; Stephen, E.; Webber, S. E.; Munk, P. *J. Polym. Sci., Part B: Polym. Phys.* **1995**, *33*, 1713.
(19) Wilhelm, M.; Zhao, C.-L.; Wang, Y.; Xu, R.; Winnik, M. A.; Mura, J.-L.; Riess, G.; Croucher, M. D. *Macromolecules* **1991**, *24*, 1033.
(20) Astafieva, I.; Zhong, X. F.; Eisenberg, A. *Macromolecules* **1993**, *26*, 7339
(21) Hurter, P. N.; Hatton, T. A. *Langmuir* **1992**, *8*, 1291.
(22) Gao, Z., Varshney, S. K., Wong S., Eisenberg, A. *Macromolecules* **1994**, *27*, 7923.
(23) (a) Zhang, L.; Eisenberg, A. *Science* **1995**, *268*, 1728. (b) Zhang, L.; Eisenberg, A. *J. Am. Chem. Soc.* **1996**, *118*, 3168. (c) Zhang, L.; Eisenberg, A. *Macromolecules* **1996**, *29*, 8805.
(24) Zhang, L., Barlow R. J., Eisenberg, A. *Macromolecules* **1995**, *28*, 6055.
(25) (a) Zhang, L.; Yu K., Eisenberg, A. *Science* **1996**, *272*, 1777. (b) Zhang, L.; Yu K., Eisenberg, A. *Langmuir* **1996**, *12*, 5980.
(26) Yu K., Eisenberg, A. *Macromolecules* **1996**, *29*, 6359.
(27) Dong, D. C.; Winnik, M. A. *Can. J. Chem.* **1984**, *62*, 2560.
(28) Kalyanasundaram, K.; Thomas, J. K. *J. Am. Chem. Soc.* **1977**, *99*, 2039.
(29) Hunter, T. F. *Chem. Phys. Lett.* **1980**, *75*, 152.
(30) Zhang, L.; Shen, H.; Eisenberg A., *J. Phys Chem. B* **1997**, *101*, 4697.
(31) Zhong, X-F.; Varshney, S. K.; Eisenberg, A. *Macromolecules* **1992**, *25*, 7160.
(32) Al-Saden, A. A.; Whately, T. L.; Florence, A. T.; *J. Colloid Interface Sci.* **1982**, *90*, 303.
(33) Anton, P.; Koberle, P.; Laschewsky, A. *Makromol. Chem.* **1993**, *194*, 1.
(34) Jacobs, P. T.; Geer, R. D.; Anacker, E. W. *J. Colloid Interface Sci.* **1972**, *39*, 611.

MA970427Z